# Chapter 4

## A Selective $^{15}$N-to-$^{1}$H Polarization Transfer Sequence for More Sensitive Detection of $^{15}$N-Choline

## 4.1 ABSTRACT

This chapter discusses selective polarization transfer from $^{15}$N to methyl $^{1}$H spins in $^{15}$N-choline. The sensitivity and information content of heteronuclear nuclear magnetic resonance is frequently optimized by transferring spin order of spectroscopic interest to the isotope of highest detection sensitivity prior to observation. This strategy was extended to $^{15}$N-choline using the scalar couplings to transfer polarization from $^{15}$N to choline's nine methyl $^{1}$H spins in high field. A theoretical analysis of a sequence using nonselective pulses showed that the optimal efficiency of this transfer is decreased by 62% as the result of competing $^{15}$N-$^{1}$H couplings involving choline's four methylene protons. A frequency-selective pulse was therefore incorporated to support evolution of only the $^{15}$N-methyl $^{1}$H coupling during the transfer period. This sequence provided a 52% sensitivity enhancement over the nonselective version in *in vitro* experiments on a sample of t hermally polarized $^{15}$N-choline in $D_2O$. Further, the $^{15}$N $T_1$ of choline in $D_2O$ was measured to be $217 \pm 38$ s, the $^{15}$N-methyl $^{1}$H coupling constant was found to be $0.817 \pm 0.001$ Hz, and the larger of choline's two $^{15}$N-methylene $^{1}$H coupling constants was found to be $3.64 \pm 0.01$ Hz. Possible improvements and applications to *in vivo* experiments using long-lived hyperpolarized heteronuclear spin order are discussed.

## 4.2 INTRODUCTION

It is now possible to routinely generate samples of certain small biomolecules with nuclear polarizations on the order of ten percent using PASADENA (parahydrogen and synthesis allow dramatically enhanced nuclear alignment) [1] or DNP (dynamic nuclear polarization) [2; 3]. These technologies show promise for clinical applications based on the *in vivo* characterization of metabolic processes on the seconds timescale. Experiments of this nature, rely on storage of the polarization on heteronuclei with long population relaxation times, such as carbonyl $^{13}C$ or quaternary $^{15}N$ nuclei, in order to minimize relaxation losses during sample delivery and to provide time for transport, binding, and metabolism. However, the sensitivity enhancement afforded by this strategy is partly lost if the final signal is also detected on a low-$\gamma$ heteronucleus. Chekmenev *et al*. [4] have proposed that optimal sensitivity can be obtained by storing polarization on a slowly-relaxing heteronuclear spin and then using an INEPT[5] sequence to coherently transfer magnetization to nearby $^{1}H$ nuclei for detection, and have demonstrated the method with two hyperpolarized reagents, 1-$^{13}$C-succinate-$d_2$ and 2,2,3,3-tetrafluoropropyl 1-$^{13}$C-propionate-$d_3$ (TFPP). Those experiments were designed assuming that the relevant $^{1}H$ and $^{13}C$ sites were 3-spin ABX systems.

Here we demonstrate an extension of this polarization transfer strategy to hyperpolarized $^{15}N$-choline, an $A_9BB'CC'X$ system of 14 spin ½ nuclei. Choline is a useful biomarker, showing significantly altered uptake and metabolism in diseased brain tissue [6] and in malignant tumor cells in the breast and prostate [7; 8]. Hyperpolarization of

$^{15}$N-choline to $(4.6 \pm 1)\%$ has been reported after two hours of DNP at 1.4 K [3]. The $^{15}$N longitudinal relaxation time of $T_1 = 120$ s in blood [3] is promising for metabolic studies.

We have investigated two INEPT-based pulse sequences for $^{15}$N-to-$^{1}$H polarization transfer in $^{15}$N-choline. The first is a nonselective refocused INEPT sequence similar to that used by Chekmenev *et al.* to transfer polarization from $^{13}$C to multiple $^{1}$H sites in succinate and TFPP [4]. While this sequence is effective, a product operator analysis shows that significantly greater sensitivity can be obtained by using a selective sequence targeting choline's nine degenerate methyl $^{1}$H spins. We therefore also present a selective refocused INEPT transfer that uses a REBURP pulse to support coherence transfer from $^{15}$N to choline's methyl $^{1}$H spins while suppressing competing transfer pathways to methylene $^{1}$H nuclei. These pulse sequences are experimentally demonstrated *in vitro* using a thermally polarized sample of $^{15}$N-choline in aqueous solution.

**4.3 THEORY**

At a given spin polarization and probe efficiency, the sensitivity of detection in an NMR experiment scales as the square of the gyromagnetic ratio of the nuclide being observed. In the case of $^{15}$N hyperpolarization, therefore, a sensitivity enhancement of $(\gamma_{^1\mathrm{H}} / \gamma_{^{15}\mathrm{N}})^2 = 97$ can be obtained by transferring to $^{1}$H for detection rather than directly observing a $^{15}$N signal, assuming unity transfer of spin angular momentum, as is closely approached within an isolated $^{15}$N-$^{1}$H spin pair with a resolved scalar coupling. Such a transfer can be achieved using refocused INEPT (Figure 4.1), the standard pulse

sequence for polarization transfer between spins with a direct scalar coupling. The effect of this sequence when applied to $^{15}$N-choline can be determined using a product operator analysis. In the following discussion the relevant $^{15}$N-$^{1}$H scalar coupling constants will be labeled $J_m$, $J_a$, and $J_b$ as indicated in Figure 4.2. Couplings between the methyl and methylene $^{1}$H spins will be unimportant and are neglected.

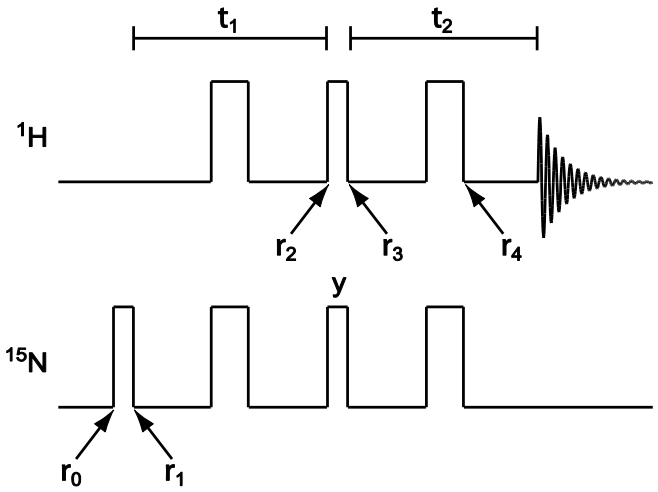


**Figure 4.1.** A refocused INEPT pulse sequence for polarization transfer from $^{15}$N to $^{1}$H for detection. Narrow (wide) rectangles denote radiofrequency pulses with a tip angle of $\pi/2$ ($\pi$). All pulses are applied along the x axis except where indicated.

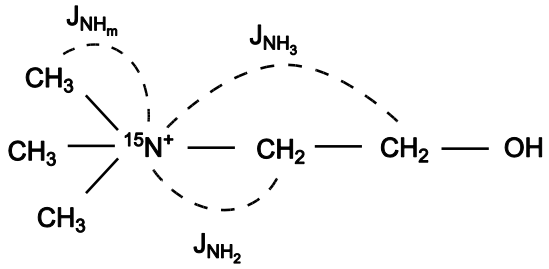


**Figure 4.2**. The structure of $^{15}$N-choline. Labels indicate the relevant $^{15}$N-$^{1}$H scalar couplings.

First, consider the effect of the sequence on the spin system of Figure 4.2, while initially neglecting the effects of the $^{15}$N-methylene $^{1}$H couplings $J_a$ and $J_b$. The system's magnetization is proportional to the dimensionless $^{15}$N spin angular momentum, with initial value normalized to $\rho_0 = S_z$. This is converted to in-phase $^{15}$N single-quantum coherence by the first $^{15}$N $(\pi/2)_x$ pulse to obtain $\rho_1 = -S_y$. This coherence evolves under the $^{15}$N-methyl $^{1}$H scalar couplings during the INEPT transfer period $\tau_1$ to produce terms that are antiphase with respect to the methyl $^{1}$H spins. The simultaneous $\pi$ pulses in the middle of $\tau_1$ refocus chemical shift evolution, leaving only the effects of couplings between $^{15}$N and each of the nine methyl $^{1}$H spins. At the end of $\tau_1$ the system's state is given by:

$$\rho_2 = -S_y \cos^9(\pi J_m \tau_1) + \sum_{i=1}^{9} 2S_x I_{iz} \cos^8(\pi J_m \tau_1)\sin(\pi J_m \tau_1)$$
$$+ \sum_{i=1}^{8}\sum_{j=i+1}^{9} 4S_y I_{iz} I_{jz} \cos^7(\pi J_m \tau_1)\sin^2(\pi J_m \tau_1) + HO.$$

Here, *HO* indicates higher-order terms, specifically single-quantum $^{15}$N coherence that is antiphase with respect to three or more $^{1}$H spins. After the transfer delay, simultaneous $^{1}$H $(\pi/2)_x$ and $^{15}$N $(\pi/2)_y$ pulses are applied:

$$\rho_3 = -S_y \cos^9(\pi\ ^2J_{N-CH_3}\tau_1) + \sum_{i=1}^{9} 2S_z I_{iy} \cos^8(\pi\ ^2J_{N-CH_3}\tau_1)\sin(\pi\ ^2J_{N-CH_3}\tau_1)$$
$$+ \sum_{i=1}^{8}\sum_{j=i+1}^{9} 4S_y I_{iy} I_{jy} \cos^7(\pi\ ^2J_{N-CH_3}\tau_1)\sin^2(\pi\ ^2J_{N-CH_3}\tau_1) + HQ.$$

The pulses convert the terms $HO$ to high-order multiple-quantum coherences, which have been abbreviated as $HQ$. At this point, $^{15}$N coherences and multiple-quantum $^{1}$H

coherences, which will not lead to observable signals at the end of the experiment, can be dropped from the density operator. This leaves only single-quantum $^{1}$H coherences that are antiphase with respect to $^{15}$N:

$$\rho_3 = \sum_{i=1}^{9} 2S_z I_{iy} \cos^8(\pi J_m \tau_1)\sin(\pi J_m \tau_1)$$

$$.\mathrm{Ny} \rightarrow$$

$$\mathrm{Nycos}(\pi \mathrm{J}\tau)\mathrm{cos}(\pi \mathrm{J}\tau)\mathrm{cos}(\pi \mathrm{J}\tau) + 2\mathrm{NxH3zcos}(\pi \mathrm{J}\tau)\mathrm{cos}(\pi \mathrm{J}\tau)\mathrm{sin}(\pi \mathrm{J}\tau) +$$

$$2\mathrm{NxH2zcos}(\pi \mathrm{J}\tau)\mathrm{sin}(\pi \mathrm{J}\tau)\mathrm{cos}(\pi \mathrm{J}\tau) + 4\mathrm{NxH2zH3zcos}(\pi \mathrm{J}\tau)\mathrm{sin}(\pi \mathrm{J}\tau)\mathrm{sin}(\pi \mathrm{J}\tau) +$$

$$2\mathrm{NxH1zsin}(\pi \mathrm{J}\tau)\mathrm{cos}(\pi \mathrm{J}\tau)\mathrm{cos}(\pi \mathrm{J}\tau) + 4\mathrm{NxH1zH2zcos}(\pi \mathrm{J}\tau)\mathrm{sin}(\pi \mathrm{J}\tau)\mathrm{sin}(\pi \mathrm{J}\tau) +$$

$$4\mathrm{NxH1zH2zsin}(\pi \mathrm{J}\tau)\mathrm{sin}(\pi \mathrm{J}\tau)\mathrm{cos}(\pi \mathrm{J}\tau) + 8\mathrm{NxH1zH2zH3zsin}(\pi \mathrm{J}\tau)\mathrm{sin}(\pi \mathrm{J}\tau)\mathrm{sin}(\pi \mathrm{J}\tau)$$

The next part of the sequence is a refocusing period of duration $\tau_2 = 1/(2J_m)$ during which the antiphase single-quantum $^{1}$H terms evolve into in-phase $^{1}$H coherence:

$$\rho_4 = -\sum_{i=1}^{9} I_{ix} \cos^8(\pi J_m \tau_1)\sin(\pi J_m \tau_1).$$

The detected $^{1}$H signal is proportional to the total magnetization of the nine methyl protons, so the dependence of the initial signal amplitude on $\tau_1$ is:

$$S_{sel} = A_{sel} 9cos^8(\pi J_m \tau_1)sin(\pi J_m \tau_1) + C. \qquad (1)$$

This expression includes a hardware-dependent proportionality constant $A_{sel}$ and a constant $C$ accounting for any DC offset in the observed signal. Equation 1 is similar to the expression derived by Doddrell *et al*. for a coherence transfer in the opposite direction, from *n* equivalent $^{1}$H spins to a heteronucleus [9]. The value of $\tau_1$ that maximizes $S_{sel}$ is given by:

$$\tau_1 = \frac{1}{\pi J_m} \tan^{-1}\left(\frac{1}{2\sqrt{2}}\right).$$

For the value $J_m = 0.82$ Hz measured experimentally for $^{15}$N-choline, the optimal transfer delay is $\tau_1 = 0.132$ s, yielding $S_{sel} = 1.873 A_{sel} + C$. The transfer function of the angular momentum from $^{15}$N to $^{1}$H or vice versa (Eq. 1) can exceed unity. The conserved quantity is the sum of the squares of the coefficients of the normalized product operators expressing the density operator. Contributions to the observable signal from choline's nine methyl $^{1}$H spins combine linearly and constructively at the optimized value of $\tau_1$.

The above calculation is readily generalized to include the effects of scalar coupling between the $^{15}$N spin and the four methylene protons ($J_a$ and $J_b$ in Fig. 2), yielding an analogous relative signal function:

$$S_{non} = A_{non} 9cos^8(\pi J_m \tau_1) sin(\pi J_m \tau_1) cos^2(\pi J_a \tau_1) cos^2(\pi J_b \tau_1) + C \qquad (2)$$

A proportionality constant $A_{non}$ and a DC offset constant C have again been included. Maximizing this function numerically for the best known values of the three coupling constants for choline, $J_m = 0.82$ Hz, $J_a = -0.57$ Hz, $J_b = 3.64$ Hz, gives an optimal transfer delay $\tau_1 = 0.233$ s, which yields a signal of $S_{non} = 0.721 A_{non} + C$.

Comparing the maximum values of $S_{sel}$ and $S_{non}$, it is apparent that the $^{15}$N-methylene $^{1}$H couplings have the effect of reducing the observable $^{1}$H signal by 62% in the idealized case of an experiment for which $A_{sel} = A_{non}$ and $C = 0$. It would clearly be advantageous to suppress these couplings. This can be achieved by replacing the $^{1}$H p

pulse in the middle of $\tau_1$ with a selective pulse tailored to invert the methyl $^1$H spins without affecting the methylene $^1$H spins.

**4.4 EXPERIMENTAL**

Data was collected on a Varian $^{UNITY}$*INOVA* spectrometer operating at a $^1$H resonance frequency of 500 MHz. The sample was prepared by dissolving 20 mg $^{15}$N-choline chloride (ISOTEC, Miamisburg, Ohio) in 700 µl $D_2O$. Refocused INEPT experiments were performed using the pulse sequence shown in Figure 4.3, which implements the selective $^{15}$N-methyl $^1$H transfer described in the theory section using a 6.695 ms $^1$H REBURP pulse [10] centered at the methyl $^1$H frequency. A time $\tau_{reb}$ = 6.4 ms, equal to the effective evolution time of the $^{15}$N-methyl $^1$H coupling during the REBURP pulse, was subtracted from the transfer delay as indicated in Fig. 3. For nonselective INEPT experiments, the REBURP was replaced with a nonselective $\pi$ pulse and $\tau_{reb}$ was set to zero.

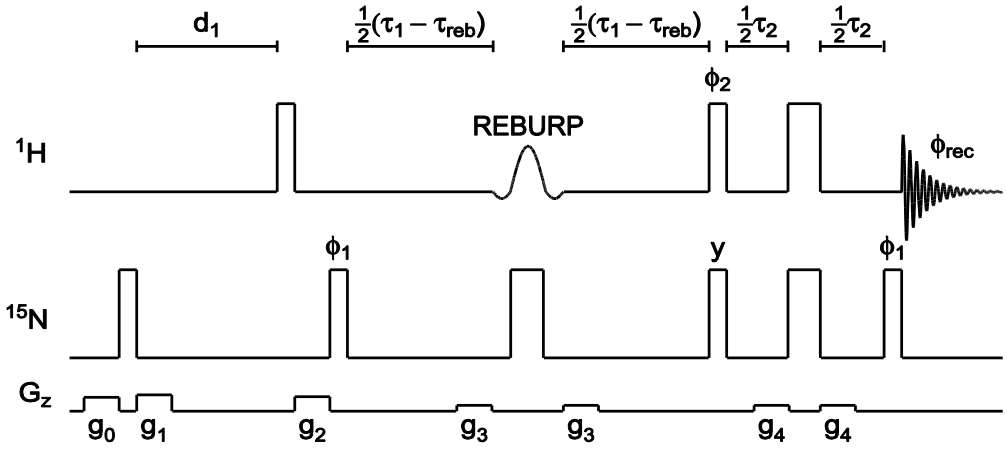


**Figure 4.3**. Selective refocused INEPT pulse sequence for coherent polarization transfer from $^{15}$N to methyl $^{1}$H in $^{15}$N-choline. Narrow (wide) rectangles denote radiofrequency pulses with a tip angle of $\pi/2$ ($\pi$), applied with $B_1$ field strengths of 23.9 kHz for $^{1}$H and 15.6 kHz for $^{15}$N. The shaped $^{1}$H pulse is a 6.695 ms REBURP [10] centered on the methyl $^{1}$H frequency. A four step phase cycle ($\varphi_1$ = x, x, x, x; $\varphi_2$ = x, y, x, y; $\varphi_{rec}$ = x, y, x, y) was used to suppress signals originating from $^{1}$H magnetization and to prevent carry over of signal from one transient to the next. A recycle delay $d_1$ of 60 s (~ 0.25 $T_1$) was used. Since it is impractical to make this delay long enough to allow full relaxation of the choline $^{15}$N spin, a purge element consisting of a $^{15}$N $\pi/2$ pulse sandwiched by gradients $g_0$ and $g_1$ is used to eliminate $^{15}$N magnetization at the start of $d_1$, ensuring a consistent starting magnetization for all experiments. A $^{1}$H purge element comprising a $^{1}$H $\pi/2$ pulse and gradient $g_2$ is used at the start of each transient. Gradients $g_3$ and $g_4$ are used to suppress coherence transfer pathways created by imperfect $\pi$ pulses.

To allow efficient testing in the absence of hyperpolarization, the sequence includes a $^{15}$N purge element before the recycle delay $d_1$ to ensure that the system reaches a consistent state at the start of each transient. This measure is necessary because it is impractical to allow full relaxation of the choline $^{15}$N spin after each transient owing to its very long $T_1$. The sequence includes a $^{15}$N $\pi/2$ pulse immediately prior to acquisition in order to purge any $^{1}$H coherence that remains antiphase with respect to $^{15}$N after the refocusing period. In the absence of this pulse, intermittent phase aberrations were observed in the methyl $^{1}$H resonance.

For $^{15}$N $T_1$ measurements by inversion-recovery, the pulse sequence of Figure 4.3 was modified by adding a $^{15}$N $\pi$ pulse and a variable recovery delay immediately before the $^{1}$H purge pulse. For these experiments, the $^{15}$N purge element before $d_1$ was removed and $d_1$ was increased to 600 s.

Data analysis was performed in MATLAB (The MathWorks, Natick, MA) using scripts developed in house. Spectral data was quantified by fitting the methyl $^{1}$H resonance to a complex Lorentzian lineshape function, except for inversion-recovery data, which was quantified by integration. A downhill simplex algorithm was used for least-squares data fitting, and uncertainties in the extracted parameters were estimated using a bootstrap Monte Carlo method [11].

The value of $\tau_{reb}$, which is subtracted from the INEPT transfer delay in order to account for evolution of the $^{15}$N-methyl $^{1}$H scalar coupling during the long REBURP pulse, was determined using a numerical simulation of the pulse sequence. Calculations

were performed in GAMMA v4.1.2 [12] in Hilbert space using a spin system of practical size, consisting of one $^{15}$N and six methyl $^{1}$H spins, with $J_m = 0.82$ Hz. The $^{1}$H resonance frequency was set to 500 MHz, and the carrier frequencies were set on resonance with the $^{15}$N and methyl $^{1}$H spins. The REBURP and the nonselective pulses were simulated with finite widths corresponding to the experimental values, and relaxation and phase cycling were neglected. The pulse sequence shown in Figure 4.3 was simulated, and the methyl $^{1}$H signal amplitude was calculated, for each of a series of values of the INEPT transfer delay $(\tau_1 - \tau_{reb})$. The signal data, shown in Figure 4.4, was then subjected to least-squares fit to a version of Eq. 1 appropriate for a system containing six methyl $^{1}$H spins and including $\tau_{reb}$ as an adjustable parameter, resulting in the value of $\tau_{reb} = 6.4$ ms used experimentally.

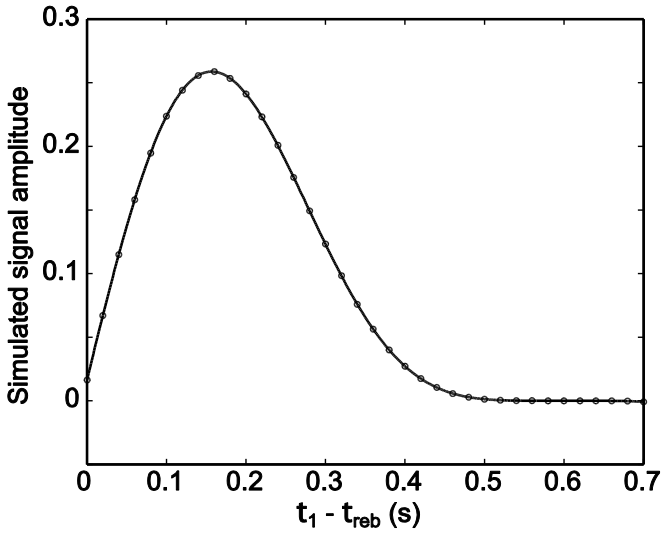


**Figure 4.4**. Numerical simulation of the selective $^{15}$N-to-$^{1}$H INEPT pulse sequence acting on a simplified spin system. Circles are simulated methyl $^{1}$H signal amplitudes for different values of the INEPT transfer delay $(\tau_1 - \tau_{reb})$. The line was calculated using a modified form of Eq. 1 with parameter values from a least-squares fit to the data. This fit was used to determine $\tau_{reb}$, the effective evolution time of the $^{15}$N-methyl $^{1}$H coupling during the sequence's REBURP pulse.

**4.5 RESULTS AND DISSCUSSION**

Figure 4.5 shows a spectrum of $^{15}$N-choline recorded using the selective $^{15}$N-to-$^{1}$H INEPT sequence of Figure 4.3, alongside a $^{15}$N-detected spectrum of the same sample recorded in a similar measurement time. It is not meaningful to compare these spectra quantitatively because they were both recorded using a probe that is optimized for direct heteronuclear observation, a factor which diminishes the sensitivity advantage of $^{1}$H detection. However, even under these unfavorable circumstances the signal-to-noise ratio is clearly much higher in the selective INEPT spectrum (Figure 4.5a) than in the $^{15}$N-detected spectrum (Figure 4.5b).

A modified version of the selective $^{15}$N-to-$^{1}$H INEPT experiment was used to measure the $^{15}$N longitudinal relaxation time of $^{15}$N-choline in $D_2O$ solution, and a value of $T_1 = (217 \pm 38)$ s was obtained (Figure 4.6). This is comparable to the value $T_1 = (285 \pm 12)$ s previously reported by Gabellieri *et al.* [3] for $^{15}$N-choline in 90% $H_2O$ / 10% $D_2O$.

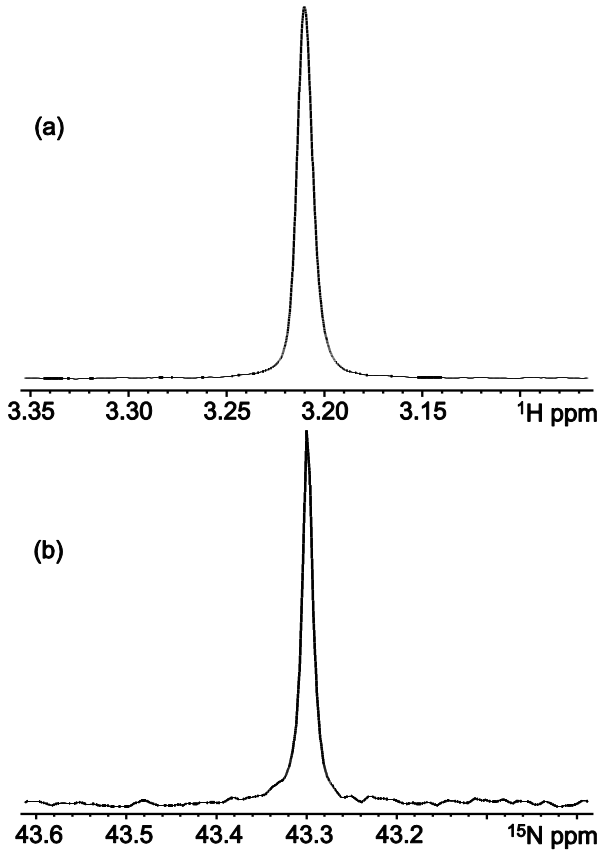


**Figure 4.5.** (a) $^{1}$H spectrum of $^{15}$N-choline recorded using the selective $^{15}$N-to-$^{1}$H INEPT sequence of Fig. 3. Only the methyl resonance is shown. (b) Single-pulse $^{15}$N spectrum of $^{15}$N-choline, recorded with tip angle $\pi/2$. Spectra (a) and (b) were each collected on the same Varian AutoX Dual Broadband probe, taking the sum of four transients with a recycle delay of 60 s. An enhancement factor of 11.0 greater sensitivity when using selective $^{15}$N-to-$^{1}$H INEPT sequence was estimated from Monte Carlo fits of (a) and (b) to Lorentzian lineshapes. The peak amplitudes were used as "signals" and the standard deviations as "noise" to construct pseudo "SNR" values for each spectrum to take into account differences in the linewidths of $^{1}$H and $^{15}$N peaks. The ratio $\frac{"SNR"_{^{1}H}}{"SNR"_{^{15}N}}$ gave the calculated enhancement factor.

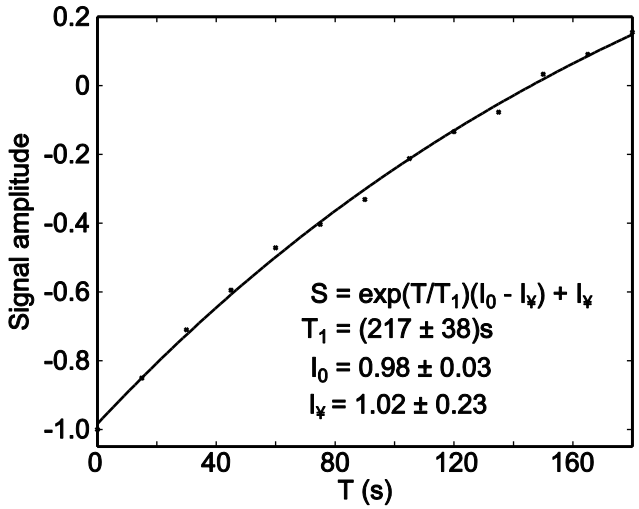


**Figure 4.6.** Measurement of the $^{15}N$ longitudinal relaxation time of $^{15}N$-choline in $D_2O$ solution using a modified version of the pulse sequence shown in Figure 3. The experiment was repeated for 13 values of the inversion-recovery delay T = 0.001, 15, 30, 45, …, 180 s. Crosses are experimental methyl $^{1}H$ signal amplitudes obtained by integrating the spectral data. The line was calculated using the indicated equation and parameter values from a least-squares fit to the data.

A series of $^{15}$N-choline $^{15}$N-to-$^{1}$H INEPT spectra were recorded using both selective and nonselective versions of the pulse sequence of Figure 3 with values of the transfer delay $\tau_1$ ranging from 6.4 ms to 700 ms. The methyl $^{1}$H signal amplitudes observed in these experiments are plotted in Figure 7. The selective INEPT sequence allows $^{15}$N-choline to be detected with 52% greater sensitivity than the nonselective sequence, comparing the maximum signal amplitude observed in each case. In the Theory section, the amplitude of the methyl $^{1}$H signal was predicted as a function of the transfer delay for the selective (Eq. 1) and nonselective (Eq. 2) experiments using a product operator analysis. By fitting the observed signal amplitudes to Eqs. 1 and 2, the optimal length of $\tau_1$ for each experiment can be determined, as well as precise values of choline's $^{15}$N-$^{1}$H coupling constants.

A simultaneous least-squares fit to both datasets yields parameter values $A_{sel} = 0.632 \pm 0.001$, $A_{non} = 1.000 \pm 0.005$, $J_m = (0.817 \pm 0.001)$ Hz, $J_b = \left(3.64 \pm 0.01\right)$ Hz, and $C = 0.000 \pm 0.001$. These values for the coupling constants agree well with ones derived from previously published $^{1}$H-$^{14}$N values: $J_m = 0.80$ Hz and $J_b = 3.61$ Hz [13]. The value of the smaller $^{15}$N-methylene $^{1}$H coupling constant was found to have a negligible effect on the fitting process, so this parameter was fixed at a reasonable value of $J_a = -0.57$ Hz.

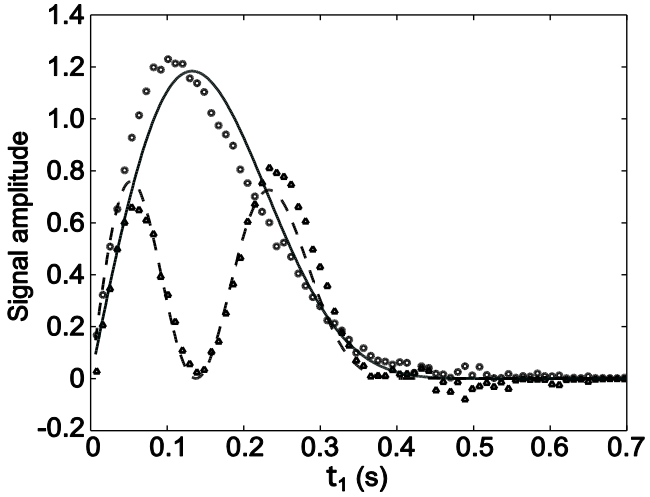


**Figure 4.7.** Amplitude of the methyl $^{1}$H signal observed in $^{15}$N-to-$^{1}$H INEPT spectra of $^{15}$N-choline using selective (circles) and nonselective (triangles) versions of the pulse sequence shown in Figure 3, as a function of the INEPT transfer period $\tau_1$. The lines were calculated using Eq. 1 (solid line) and Eq. 2 (dashed line) with parameter values from a least-squares fit to the data.

Note that, for experiments using the selective and nonselective versions of the pulse sequence of Figure 3 on the same spectrometer hardware and sample, the constants $C$ in Eqs. 1 and 2 should be the same, but $A_{sel}$ may be smaller than $A_{non}$ due to signal losses during the selective sequence's REBURP pulse. Comparing the values of $A_{sel}$ and $A_{non}$ from the least squares fit it appears that 36% of the signal is lost in this way. This can be attributed in part to miscalibration of the REBURP pulse. A three pulse sequence ($\pi/2$ - REBURP - $\pi/2$) was used to calibrate the REBURP pulse by seeking pulse width and power parameters that gave the best null signal. It would be more appropriate to choose a calibration sequence that uses the REBURP pulse for inversion, as it is used in the selective INEPT sequence, rather than for refocusing. Also, a sequence with a larger number of pulses would be preferable, so that the cumulative effects of $B_1$ inhomogeneity would be comparable in the calibration sequence and the selective INEPT sequence.

We have presented a pulse sequence that suppresses the effects of the four methylene protons on the INEPT transfer from $^{15}$N to methyl $^{1}$H in $^{15}$N-choline. Note that the same result can be achieved by selective deuteration of $^{15}$N-choline. This approach might provide the additional benefit of increasing the molecule's $^{15}$N longitudinal relaxation time and would be an option for DNP experiments. However, the present selective recoupling strategy is clearly advantageous for $^{15}$N-choline hyperpolarization using PASADENA. In these experiments, two of the methylene $^{1}$H spins derive from a parahydrogen molecule which reacts with an unsaturated precursor to initiate the hyperpolarization process. Although deuteration of the alkene precursor

can remove two of the methylene $^{1}$H spins, those which supply the spin order cannot be eliminated.

The success of this selective coherence transfer strategy in $^{15}$N-choline has clear implications for studies of other hyperpolarized small biomolecules. By directing the spin order to a subset of the possible detection spins, sensitivity is improved. The recoupling strategy demonstrated here accomplishes this by way of a frequency selective $\pi$ pulse, which simplifies, and often shortens, the polarization transfer step. Similar selective INEPT sequences could be used to improve the sensitivity of the $^{13}$C-to-$^{1}$H polarization transfer experiments demonstrated by Chekmenev *et al.* in hyperpolarized TFPP [4] by directing the spin order to one of the resolved $^{1}$H sites.

The selective $^{15}$N-choline transfer presented here also has potentially useful applications to thermally polarized *in vivo* $^{15}$N spectroscopy. Pulse sequences can be devised to transfer methyl $^{1}$H polarization to $^{15}$N for an encoding period and then back to methyl $^{1}$H for detection. Such sequences would benefit from choline's long $^{15}$N $T_1$ while making use of the strong thermal polarization of the nine methyl $^{1}$H spins. This strategy could be used to resolve species such as choline and phosphocholine by $^{15}$N-$^{1}$H correlation spectroscopy, or even to study the metabolic interconversion of choline and related compounds using a sequence with a longitudinal $^{15}$N period for chemical exchange.

## 4.6 CONCLUSION

As part of a strategy to improve the sensivity of *in vivo* experiments on hyperpolarized small biomolecules, we have investigated INEPT pulse sequences for the transfer of magnetization from $^{15}$N to the methyl $^{1}$H spins in $^{15}$N-choline. Product operator analysis of a simple refocused INEPT sequence shows that the optimized efficiency of this transfer is diminished by 62% by the action of competing couplings between $^{15}$N and choline's methylene $^{1}$H spins. A selective INEPT sequence, using a $^{1}$H REBURP pulse to suppress undesired couplings during the transfer period, was devised and tested *in vitro* on a thermally polarized $^{15}$N-choline sample. It was demonstrated that the selective INEPT sequence leads to a 52% stronger methyl $^{1}$H signal than the nonselective version.

## 4.7 ACKNOWLEGEMENTS

This work was done in collaboration with Jason E. Ollerenshaw, Valerie A. Norton, and Daniel P. Weitekamp. It was supported by the Beckman Institute pilot program, "Spin-Polarized Molecules for Structural and Systems Biology." JEO was supported by a Postdoctoral Fellowship from the Natural Sciences and Engineering Research Council of Canada.

## 4.8 REFERENCES

[1] E.Y. Chekmenev, J. Hovener, V.A. Norton, K. Harris, L.S. Batchelder, P. Bhattacharya, B.D. Ross, and D.P. Weitekamp, PASADENA Hyperpolarization of Succinic Acid for MRI and NMR Spectroscopy. Journal of the American Chemical Society 130 (2008) 4212-4213.

[2] K. Golman, Metabolic imaging by hyperpolarized 13C magnetic resonance imaging for in vivo tumor diagnosis. Cancer Research 66 (2006) 10855.

[3] C. Gabellieri, S. Reynolds, A. Lavie, G.S. Payne, M.O. Leach, and T.R. Eykyn, Therapeutic target metabolism observed using hyperpolarized $^{15}$N choline. J. Am. Chem. Soc. 130 (2008) 4598-4599.

[4] E.Y. Chekmenev, V.A. Norton, D.P. Weitekamp, and P. Bhattacharya, Hyperpolarized $^{1}$H NMR employing low g nucleus for spin polarization storage. J. Am. Chem. Soc. 131 (2009) 3164-3165.

[5] R.F. Gareth A. Morris, Enhancement of Nuclear Magnetic Resonance Signals by Polarization Transfer. Journal of the American Chemical Society 101 (1979) 763-762.

[6] Y. Boulanger, M. Labelle, and A. Khiat, Role of phospholipase $A_2$ on the variations of the choline signal intensity observed by $^{1}$H magnetic resonance spectroscopy in brain diseases. Brain Res. Rev. 33 (2000) 380-389.

[7] R. Katz-Brull, D. Seger, D. Rivenson-Segal, E. Rushkin, and H. Degani, Metabolic markers of breast cancer: enhanced choline metabolism and reduced choline-ether-phospholipid synthesis. Cancer Res. 62 (2002) 1966-1970.

[8] E. Sutinen, M. Nurmi, A. Roivainen, M. Varpula, T. Tolvanen, P. Lehikoinen, and H. Minn, Kinetics of [$^{11}$C]choline uptake in prostate cancer: a PET study. Eur. J. Nucl. Med. Mol. Imaging 31 (2004) 317-324.

[9] D.M. Doddrell, D.T. Pegg, W. Brooks, and M.R. Bendall, Enhancement of $^{29}Si$ or $^{119}Sn$ NMR signals in the compounds $M(CH_3)_nCl_{4-n}$ (M = Si or Sn, R = 4, 3, 2) using proton polarization transfer. Dependence of the enhancement on the number of scalar coupled protons. J. Am. Chem. Soc. 103 (1981) 727-728.

[10] H. Geen, and R. Freeman, Band-selective radiofrequency pulses. J. Magn. Reson. 93 (1991) 93-141.

[11] W.H. Press, S.A. Teukolsky, W.T. Vetterling, and B.P. Flannery, Numerical Recipes in C: The Art of Scientific Computing $2^{nd}$ edition, Cambridge University Press, Cambridge, UK, 1992.

[12] S.A. Smith, T.O. Levante, B.H. Meier, and R.R. Ernst, Computer simulations in magnetic resonance. An object-oriented programming approach. J. Magn. Reson. A106 (1994) 75-105.

[13] V. Govindaraju, K. Young, and A.A. Maudsley, Proton NMR chemical shifts and coupling constants for brain metabolites. NMR Biomed. 13 (2000).